

## INVASIVENESS OF OPTICAL MAGNETIC FIELD PROBES WITH A LOOP ANTENNA ELEMENT

Satoru Arakawa<sup>\*</sup>, Eiji Suzuki<sup>\*</sup>, Hiroyasu Ota<sup>\*</sup>, Kenichi Arai<sup>\*,\*\*</sup>, and Risaburo Sato<sup>\*</sup>

<sup>\*</sup>Sendai EMC Research Center, Telecommunications Advancement Organization of Japan

<sup>\*\*</sup>Research Institute of Electrical Communication, Tohoku University

E-mail: arakawa@emc-rc.tao.go.jp

**Abstract:** Electromagnetic field probes inevitably change the original field distribution to some extent when they are positioned close to a device. That change affects measurement accuracy and the device operation. We have developed optical magnetic field probes, which comprise a loop antenna element and an electro-optic crystal, to perform magnetic near-field measurement with high accuracy in the GHz frequency band. This study analyzes the invasiveness of the optical magnetic field probes quantitatively by experiment and finite difference time domain (FDTD) method simulation. We found that the electromagnetic field disturbance is reduced greatly by eliminating a metallic cable. In addition, the optical magnetic field probes were found to offer the advantage of accurate measurement.

**Key words:** Magnetic near-field measurement, Probe, Loop antenna, Electro-optical effect, Invasiveness, Finite difference time domain (FDTD) method

### 1. Introduction

Probes with an attached loop antenna element at the end of a coaxial cable are used commonly for magnetic near-field measurement. Such probes provide an output that is proportional to magnetic field intensity when the loop perimeter is sufficiently small in comparison to the wavelength of the electromagnetic wave. However, in frequency bands for which the perimeter of a loop becomes about 1/10 or more of the wavelength, a remarkable influence of the electric field appears. Shielded loop probes were devised as structures that can suppress the voltage induced by an electric field; they are widely used for magnetic field measurement at comparatively high frequency bands [1]. Recently, shielded loop probes of multilayered board structure have been proposed along with studies intended toward their miniaturization and higher spatial resolution [2].

Moreover, probes inevitably change the surrounding electromagnetic field distribution when they are positioned close to the device during magnetic near-field measurement. Such disturbance affects the measurement accuracy and operation of devices. Such invasiveness of probes has become an important issue recently [3]–[5].

We have analyzed the following problems to perform magnetic near-field measurement with high accuracy in the GHz frequency band.

- (1) Disturbance of electromagnetic fields by the measurement system itself, such as the probe and the metallic cable for signal transmission.
- (2) Influence on measurement of magnetic fields.
- (3) Influence on operation of the device.

We found that the invasive impact on the surrounding field that is to be measured can be reduced greatly by eliminating the metallic cable component [6]. Moreover, we are developing optical magnetic field probes that have no metallic cables: they consist of a loop antenna element and an electro-optic crystal [7].

This study quantitatively evaluates invasiveness of optical magnetic field probes by experimentation and FDTD method simulation. We verified that optical magnetic field probes provide accurate measurement.

### 2. Optical Magnetic Field Probe

Fig. 1 shows the measurement system of the optical magnetic field probe. It consists of a loop element formed on the dielectric board and an electro-optic crystal (LiNbO<sub>3</sub>) inserted between electrodes of a loop terminus portion. A continuous-wave laser beam guided through an optical fiber passes through an optical circulator and a lens; the beam finally enters the LiNbO<sub>3</sub> perpendicularly to the c-axis of the LiNbO<sub>3</sub>. A magnetic field penetrating the loop aperture produces a voltage between both ends of the LiNbO<sub>3</sub> electrodes according to Faraday's law of electromagnetic induction. The refractive indices of the LiNbO<sub>3</sub> change proportionally to the voltage because of the linear electro-optical effect (the Pockels effect). Therefore, the phase modulation of the beam reflected in the bottom of LiNbO<sub>3</sub> is carried out. The beam goes through the circulator, waveplates, and a polarizer to a photoreceiver. The polarizer converts the phase modulation into intensity modulation. Optical intensity is changed to the corresponding electrical signal at the photoreceiver. A spectrum analyzer processes the resultant electrical signal.

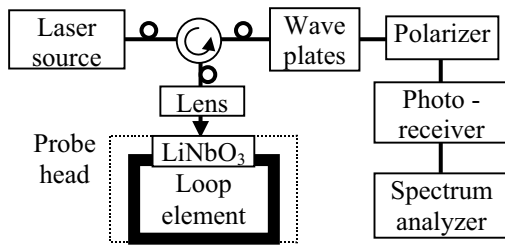


Fig. 1 Measurement system.

**3. Disturbance of Electromagnetic Fields**

We performed magnetic field distribution measurement above a microstrip line (MSL) using the optical magnetic field probe. When the probe is positioned close to the MSL, it inevitably alters the surrounding field that is to be measured. This disturbance was evaluated by FDTD method simulation.

**3.1. Analysis Model for Simulation**

Fig. 2 shows the analytical model for FDTD simulation. It comprises a loop element ( $4.5 \times 4.5$  mm aperture, 1.0-mm-width pattern) formed on the dielectric board ( $\epsilon_r = 4.8$ ) and one LiNbO<sub>3</sub> electro-optic crystal ( $0.5 \times 0.5 \times 0.8$  mm,  $\epsilon_r = 28$ ) inserted between electrodes of a loop terminus portion. The probe was set parallel to the MSL which had a 1.0-mm-width line with a 0.6-mm-thickness dielectric board ( $\epsilon_r = 4.8$ ). The space between the MSL and the bottom of the loop element was maintained at 0.5 mm.

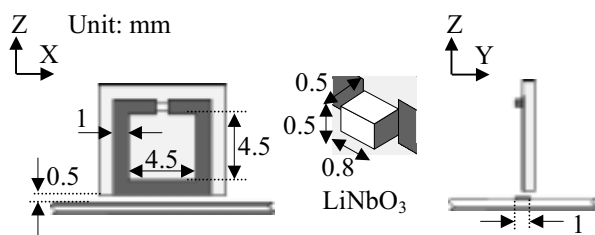


Fig. 2 Optical magnetic field probe.

Analysis of a shielded loop probe connected to a metallic cable also performed to provide comparison to conventional magnetic field probes. Fig. 3 shows the analytical model of the shielded loop probe. It has a three-layer structure in which a dielectric board ( $\epsilon_r = 4.8$ ) is sandwiched between the GND layer ( $4.5 \times 4.5$  mm aperture, 1.0-mm-width pattern) and the signal line (0.6-mm-width pattern). The signal line was connected with the GND layer through a via. The metallic cable ( $Z_0 = 50 \Omega$ ) had a rectangular coaxial structure and the terminus side was in contact with perfectly matched layer (PML) as absorbing boundary conditions.

**3.2. Intensity Distribution Change**

We verified the intensity distribution change of each axis direction components of magnetic field and the electric field. The MSL was fed sinusoidal voltage 0.708 V (10 dBm) at 1 GHz.

Fig. 4 shows the situation of intensity distribution change of the  $H_y$  component of a magnetic field. Although the  $H_y$  distribution changes greatly along a metallic cable when the shielded loop probe has been positioned, it turns out that this influence decreases in the case of the optical magnetic field probe.

Similarly from the result about electric field, when each probe is positioned, electric field components change along metallic elements. Moreover, electric field distributions change greatly along the metallic cable.

The above results indicate that electromagnetic field disturbance can be reduced by eliminating the metallic cable and performing signal transmission by optical fiber.

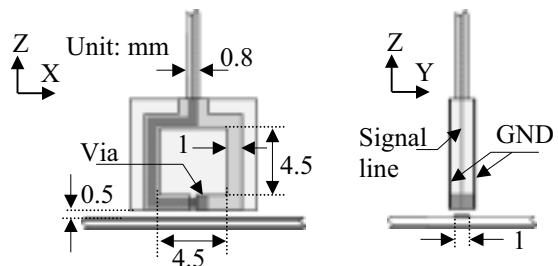


Fig. 3 Shielded loop probe.

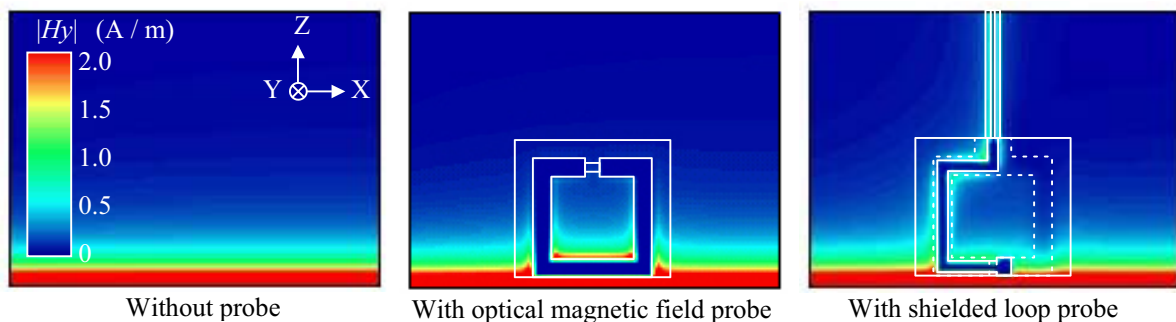


Fig. 4 Y-axis component of magnetic field distribution change caused by the probes. Analysis result by FDTD method simulation. Excitation voltage of MSL is 0.708 V (10 dBm) at 1 GHz.

#### 4. Influence on Probe Output

It is necessary to suppress the output influenced by an electric field to perform magnetic near-field measurement with high accuracy. We next verified magnetic field detection characteristics of an optical magnetic field probe.

Fig. 5 shows the experimental setting. The MSL was matched to  $50\ \Omega$  and was powered at 10 dBm at 1 GHz. The probe was set parallel ( $0^\circ$  and  $180^\circ$ ) and orthogonal ( $90^\circ$  and  $270^\circ$ ) to the MSL. The space between the MSL and the bottom of the loop element was maintained at 0.5 mm. The probe was scanned in the MSL width direction.

##### 4.1. Measurement of Magnetic Field Distribution above the MSL

We performed intensity distribution measurement of the  $H_y$  component of the magnetic field which penetrates a loop when the probe is set parallel to the MSL.

Fig. 6 shows experimental results using the optical magnetic field probe. The width of the distribution at the position 3 dB from below the maximum value just above the MSL, was about 1.6 mm. The width of the distribution at the minimum value was about 6.0 mm. The simulation value was computed from the average magnetic field intensity of  $H_y$  component in the loop aperture, which was calculated for the case without a probe. These results demonstrate that the optical magnetic field probe performed the measurement of the magnetic field distribution with sufficient accuracy.

Fig. 7 shows experimental results under the shielded loop probe. The width of a distribution at the position 3 dB from below the maximum value was about 2.4 mm; at the minimum value was about 8.0 mm. Moreover, the difference of the output maximum was about 2 dB, even though  $0^\circ$  and  $180^\circ$  settings have about the same relative position of the loop aperture. The causes are inferred to be the reduced spatial resolution engendered by the thickness of the multilayered structure and the altered output of the electric field.

##### 4.2. $H_{max} / H_{min}$ Ratio of the Optical Magnetic Field Probe

The loop element receives the maximum amount of magnetic flux under the parallel setting. On the other hand, the loop element receives no magnetic flux under the orthogonal setting. The outputs under the parallel and orthogonal setting are  $H_{max}$  and  $H_{min}$ , respectively.  $H_{min}$  outputs are not desirable for magnetic field probes because no magnetic flux penetrates the loop aperture. Therefore, we verified the  $H_{max} / H_{min}$  ratio of the probe.

Fig. 6 shows experimental results using the optical magnetic field probe: just above MSL, the  $H_{max} / H_{min}$

ratio was about 35 dB; the  $H_{max} / H_{min}$  ratio was about 23 dB at the maximum under each setting.

Fig. 7 shows experimental results for the shielded loop probe: just above MSL, the  $H_{max} / H_{min}$  ratio was about 25 dB; at the maximum under each setting, the  $H_{max} / H_{min}$  ratio was about 19 dB. Moreover, results of  $90^\circ$  and  $270^\circ$  showed an asymmetrical distribution because the structure of the shielded loop probe has slight electrical asymmetry. In addition, a part of voltage induced in the metallic cable by the electric field becomes mixed with the output.

The optical magnetic field probe can demonstrably improve the  $H_{max} / H_{min}$  ratio and can allow more accurate magnetic field measurement.

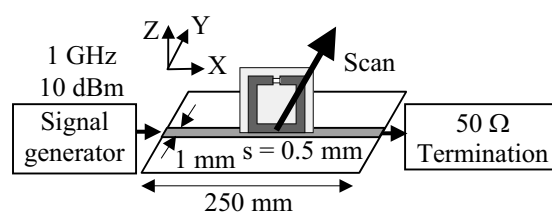


Fig. 5 Experimental setting.

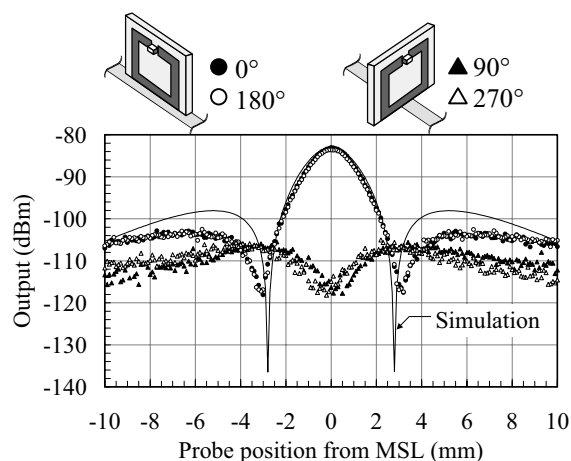


Fig. 6 Electromagnetic field distribution above MSL. Experimental results using the optical magnetic field probe.

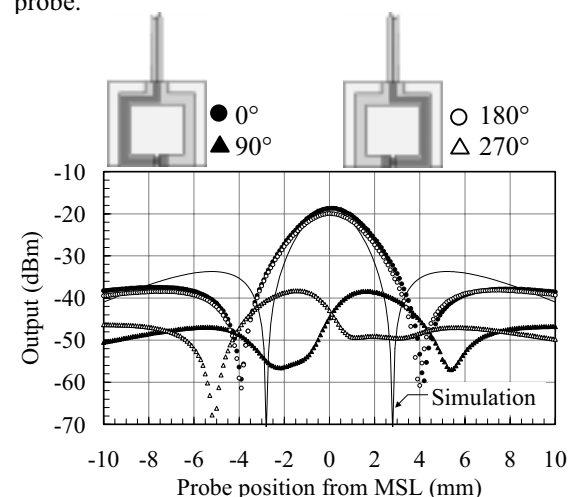


Fig. 7 Electromagnetic field distribution above MSL. Experimental results using the shielded loop probe.

5. Influence on Operation of MSL

Positioning a probe closer to a device can improve sensitivity and spatial resolution during measurement, but such positioning affects the operation of a device. We assessed that influence on MSL transmission characteristics.

The probe was set parallel to the MSL. Its position was varied in the height direction, where  $s$  ( $= 0.1 \text{ mm} \sim 1.5 \text{ mm}$ ) is the space between the MSL and the probe. The transmission coefficient of the MSL,  $S_{21}$ , was measured by the vector network analyzer in this state. We performed an identical experiment to that for the shielded loop probe connected to the spectrum analyzer.

Fig. 8 shows those experimental results. The optical magnetic field probe indicates less influence on  $S_{21}$  than the shielded loop probe below 3 GHz. Moreover, even when the optical magnetic field probe was set to  $s = 0.1 \text{ mm}$ , the influence was 0.2 dB or less. The dip at around 3.6 GHz is based on resonant frequency of the optical magnetic field probe.

Fig. 9 shows the relation between  $S_{21}$  of the MSL and the space at 1 GHz.

The above result indicates that the optical magnetic field probe, which eliminated the metal cable and reduced the metal element, can reduce the MSL influence on operation.

6. Conclusion

This study analyzed disturbance to an electromagnetic field caused by the probe and the metallic cable for signal transmission in the GHz frequency band. Results verified magnetic field detection characteristics of the probe and the influence on MSL operation. Results confirm that the optical magnetic field probe provides highly accurate measurement.

References

[1] J.D. Dyson, "Measurement of Near Fields of Antenna and Scatterers," IEEE Trans. A.P., Vol. AP-21, No. 4, Jul. 1973.  
 [2] M. Yamaguchi, S. Yabukami, and K.I. Arai, "A New Permeance Meter Based on Both Lumped Elements / Transmission Line Theories," IEEE Trans. Magn., Vol. 32, No. 5, pp. 4941-4943, Sep. 1996.  
 [3] T. Nagatsuma, T. Shibata, E. Sano, and A. Iwata, "Subpicosecond sampling using a noncontact electro-optic probe," J. Appl. Phys., 66, No. 9, pp. 4001-4009, Nov. 1989.  
 [4] X. Wu, D. Conn, J. Song, and K. Nickerson, "Invasiveness of LiTaO<sub>3</sub> and GaAs Probes in External E-O Sampling," J. Lightwave Technol., Vol. 11, No. 3, pp. 448-454, Mar. 1993.  
 [5] R.M. Reano, K. Yang, L.P.B. Katehi, and J.F. Whitaker, "Simultaneous Measurements of Electric and Thermal Fields Utilizing an Electrooptic Semiconductor Probe," IEEE Trans. Microwave

Theory Tech., Vol. 49, No. 12, pp. 2523-2531, Dec. 2001.

[6] S. Arakawa, H. Ota, and K.I. Arai, "An Analysis of Electromagnetic Field Distribution Change by Magnetic Field Probes in the Near Field Measurement," IEICE Tech. Report, EMCJ2002-20, pp. 25-30, Jun. 2002.

[7] E. Suzuki, T. Miyakawa, H. Ota, K.I. Arai, and R. Sato, "Characteristics of an optical magnetic probe consisting of a loop antenna element and a bulk electro-optic crystal," Proc. EMC Zurich 2003, pp. 61-64, 2003.

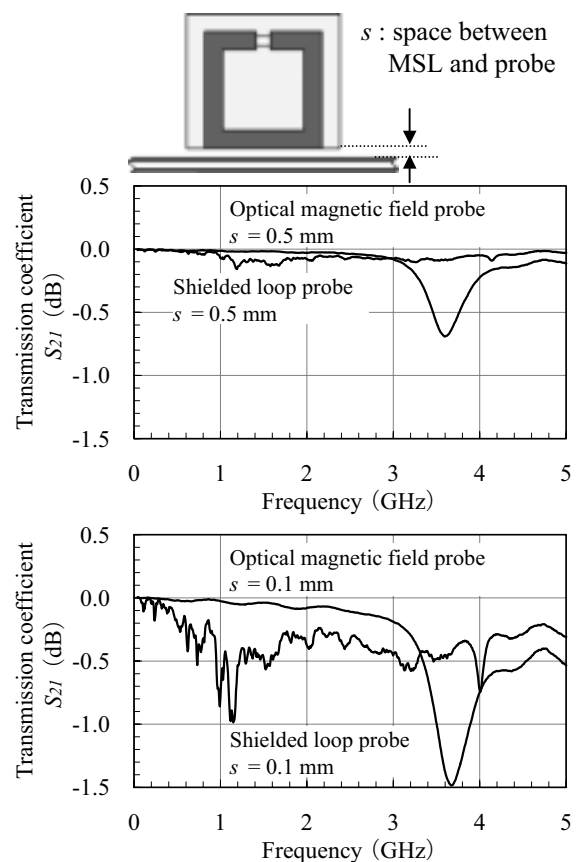


Fig. 8 Transmission coefficient  $S_{21}$  of the MSL using optical magnetic field probe and shielded loop probe.

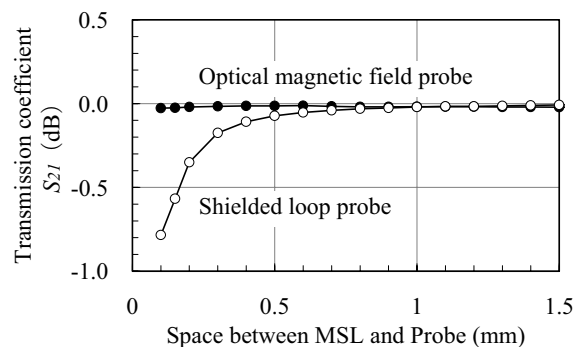


Fig. 9 Transmission coefficient  $S_{21}$  of the MSL and space between MSL and probes, at 1 GHz.